Understanding Volume Estimation Uncertainty of Lakes and Wetlands Using Satellites and Citizen Science

Shahzaib Khan, Faisal Hossain, Tamlin Pavelsky, Grant M. Parkins, Megan Rodgers Lane, Angélica M. Gómez, Sanchit Minocha, Pritam Das, Sheikh Ghafoor, Md. Arifuzzaman Bhuyan, Md. Nazmul Haque, Preetom Kumar Sarker, Partho Protim Borua, Jean-Francois Cretaux, Nicolas Picot, Vivek Balakrishnan, Shakeel Ahmad, Nirakar Thapa, Rajan Bhattarai, Faizan-ul Hasan, Bareerah Fatima, Muhammad Ashraf, Shahryar Khalique Ahmad, and Arthur Compin

***Abstract*—We studied variations in the volume of water stored in small lakes and wetlands using satellite remote sensing and lake water height data contributed by citizen scientists. A total of 94 water bodies across the globe were studied using satellite data in the optical and microwave wavelengths from Landsat 8, Sentinel-1, and Sentinel-2. The uncertainty in volume estimation as a function of geography and geophysical factors, such as cloud cover, precipitation, and water surface temperature, was studied. The key finding that emerged from this global study is that uncertainty is highest in regions with a distinct precipitation season, such as in the monsoon dominated South Asia or the Pacific Northwestern region of the USA. This uncertainty is further compounded when small lakes and wetlands are seasonal with alternating land use as a water body and agricultural land, such as the wetlands of Northeastern Bangladesh. On an average, 45% of studied lakes could be estimated of their volume change with a statistical significant uncertainty that is less than the expected volume in South Asia. In North America, this statistically significant uncertainty in volume estimation was found to be around 50% in lakes eastward of the 108th meridian with lowest uncertainty found in lakes along the East coast of the USA. The article provides a baseline for understanding the current state of the art in estimating volumetric change of lakes and wetlands using citizen science in anticipation of the recently launched Surface Water and Ocean Topography Mission.**

***Index Terms*—Citizen science, lakes, remote sensing, satellites, Surface Water and Ocean Topography (SWOT), wetlands.**

Manuscript received 10 June 2022; revised 12 January 2023 and 11 February 2023; accepted 25 February 2023. Date of publication 28 February 2023; date of current version 9 March 2023. This work was supported by the NASA under Grant 80NSSC21K0854 "Lake Observations from Citizen Scientists and Satellites: Validation of Satellite Altimetry to Support Hydrologic Science" (awarded to author Dr. Tamlin Pavelsky, University of North Carolina). *(Corresponding author: Faisal Hossain.)*

Shahzaib Khan, Faisal Hossain, Sanchit Minocha, and Pritam Das are with the Department of Civil and Environmental Engineering, University of Washington, Seattle, WA 98195 USA (e-mail: skhan7@uw.edu; fhossain@uw.edu; msanchit@uw.edu; pdas47@uw.edu).

Tamlin Pavelsky, Grant M. Parkins, Megan Rodgers Lane, and Angélica M. Gómez are with the Earth Marine and Environmental Science Department, University of North Carolina, Chapel Hill, NC 27599 USA (e-mail: pavelsky@unc.edu; parkins@unc.edu; megan.lane@unc.edu; amgomez@live.unc.edu).

Sheikh Ghafoor is with the Tennessee Technological University, Cookeville, TN 38505 USA (e-mail: sghafoor@tntech.edu).

Md. Arifuzzaman Bhuyan, Md. Nazmul Haque, Preetom Kumar Sarker, and Partho Protim Borua are with the Bangladesh Water Development Board, Dhaka 1215, Bangladesh (e-mail: arif81_bwdb@yahoo.com; nazmul.bwdb10@gmail.com; pksarker070@gmail.com; dhrubo.06@gmail.com).

Jean-Francois Cretaux and Nicolas Picot are with the LEGOS, Université de Toulouse, CNES, CNRS, IRD, Toulouse, France (e-mail: jean-francois.cretaux@cnes.fr; nicolas.picot@cnes.fr).

Vivek Balakrishnan is with the Centre for Water Resources Development and Management, Kerala 673571, India (e-mail: vivek@cwrdm.org).

Shakeel Ahmad is with the Aligarh Muslim University, Aligarh 202001, India (e-mail: shakeelamdgeol@gmail.com).

Nirakar Thapa and Rajan Bhattarai are with the Department of Hydrology and Meteorology, Kathmandu 44600, Nepal (e-mail: nirakarjung48@gmail.com; rajanbhattarai@yahoo.com).

Faizan-ul Hasan, Bareerah Fatima, and Muhammad Ashraf are with the Pakistan Council of Research in Water Resources, Islamabad, Pakistan (e-mail: faizan_ul_hasan@hotmail.com; breerahftm@gmail.com; muhammad_ashraf63@yahoo.com).

Shahryar Khalique Ahmad is with the NASA Hydrological Sciences Branch, Goddard Space Flight Center, Greenbelt, MD 20771 USA (e-mail: shahryarkhalique.ahmad@nasa.gov).

Arthur Compin is with the LEF, Toulouse, France (e-mail: arthur.compin@univ-tlse3.fr).

Digital Object Identifier 10.1109/JSTARS.2023.3250354

I. Introduction

WATER bodies, such as small lakes (i.e., those smaller than 100 km^2) and wetlands, provide vital functions for ecosystems and sustain biodiversity. Globally, wetlands cover an area of 1.2 billion hectares, which is equivalent to the area of Canada [1]. Downing et al. [2] claimed that the total surface area of natural and artificial lakes is over 4.6 million km^2, which translates to about 117 million water bodies [3]. These water bodies act as biological supermarkets, groundwater recharge, and discharge points, and they provide both water and nutrients necessary for crop production. Wetlands and small lakes also support flood control and ecotourism. According to Global Wetland Outlook (Ramsar Convention, 2021), wetlands have been rapidly declining. Approximately 35% of the world's wetlands have been disappearing since 1970 [1]. While there are various physical drivers that affect the behavior of wetlands and small lakes, the most critical among them, other than perhaps direct human management, is likely changing patterns of weather, hydrology, and climate [1].

In recent years, our ability to track the extent of small lakes and wetlands has increased manifold. Lehner and Döll [4] developed the Global Lakes and Wetlands Database (GLWD), which

provides the maps and water surface area of the lake, wetlands, reservoirs, and rivers. For lakes, GLWD was superseded by the HydroLAKES database [5], which mapped about 1.4 million lakes larger than 0.1 km^2. A study by Sheng et al. [6] mapped 7.7 million lakes that are larger than 0.004 km^2. Meanwhile, Verpoorter et al. [3] used satellite imagery to identify more than 117 million lakes globally. Hu et al. [7] studied the areal extent of the wetlands and lakes by developing a new index (precipitation topographic wetness index). However, despite this improved understanding of the location and extent of small lakes and wetlands, understanding of the physical behavior of wetlands and lakes around the world remains limited, especially in developing regions. Specifically, we understand very little about how volumetric changes of lakes and wetlands modulate over time and as a function of climate, season, or geographic region. A primary reason for this gap is the paucity of *in-situ* lake and wetland gauges relative to the widespread presence of lakes and wetlands around the globe. Unlike for rivers, there are no major national or international repositories dedicated to storing *in-situ* lake level data. Even in developed countries, such data are limited—for example, the U.S. Geological Survey gauges more than 10 000 rivers but only a few hundred lakes.

Studying volumetric changes at a global scale is therefore not feasible using limited *in-situ* gauges given the remoteness of numerous water bodies and lack of economic or institutional resources to maintain an *in-situ* measurement network. Studying wetlands and small lakes using satellite remote sensing is only cost-effective and feasible way to understand the volumetric change of water bodies on a global scale [8], [9]. Most studies that aim to do so use different sensors to study surface water extent and water surface elevation, which, in combination, allow estimation of volume change. Detection of the surface water extent and elevation can be performed with sensors of different resolutions and electromagnetic wavelengths. Coarser spatial resolution sensors, such as NOAA/AVHRR and Moderate Resolution Imaging Spectroradiometer (MODIS), have low spatial accuracy but high temporal resolution and coverage, and are often used to study large lakes [10]. Medium spatial resolution sensors, with a resolution of around 10–30 m, are widely used in studies of smaller lakes [3]. A few examples for medium resolution are the Landsat series, Sentinel 2, and Advanced Spaceborne Thermal Emission and Reflection Radiometer. High spatial resolution sensors, such as Planet, RapidEye, and IKONOS, have a resolution around 1–5 m, but they are not freely available. The type and nature of water bodies that can be studied with reasonable accuracy usually depend on the pertinent resolution and sampling frequency of sensor data that are available.

In recent years, studies have shown that multisensor approaches combining optical and SAR data to measure inundation extent are often more robust [11]. Researchers have come up with various indices like modified normalized difference water index (MNDWI) [12], normalized difference Water index [13], and techniques like dynamic surface water extent (DSWE) [14] and angle looking SAR. Optical satellites like the Landsat series [14], [15], [16], MODIS sensors onboard the National Aeronautics and Space Administration (NASA) Terra and Aqua satellites [17], and Visible Infrared Imaging Radiometer Suite onboard Suomi National Polar-orbiting Partnership [18] can be used to study water surface area and volume of water stored. However, a major drawback of optical satellites is that they cannot penetrate clouds. To overcome the issue of cloud cover, synthetic aperture radar (SAR) can be used with an understanding of the proper threshold on backscattering to detect water surfaces [19]. However, SAR may not always be accurate because other smooth surfaces and shadowed areas share almost identical scattering properties with water surfaces. For example, bare soils can sometimes create false-positive cases [20]. Despite such a wide range of available techniques, the uncertainty of surface water area and hence volume estimation due to the choice of methods has not been rigorously studied for lakes and wetlands. Understanding these uncertainties is challenging yet important. It is challenging due to cloud cover and seasonally contrasting environments. For example, freezing/thawing of lakes in higher latitudes can make detection of variations in volume difficult [21], [22]. Similarly, lake area cannot be regularly detected due to extensive cloud cover, for example, during months-long monsoon seasons.

Both optical and microwave angle-looking sensors can only estimate the area of the water bodies. On the other hand, satellite altimeters, such as Jason 3, Sentinel 3, and SARAL/AltiKa, provide water surface elevation [23]. Baup et al. [24] developed three independent approaches to estimate the lake: volume high-resolution image-based volume, altimetry-based volume, and altimetry and high-resolution-based volume changes. Duan and Bastiaanssen [25] and Cretaux et al. [26] have used a combination of lake extent and water level at different dates in order to build hypsometry relationship, which was then used to calculate lake extent and level simultaneously using satellite altimetry measurements. The uncertainty in elevations from altimeters can vary from a few centimeters for large water bodies to tens of centimeters for small water bodies [27]. The limitation of altimeters is the limited spatial sampling due to the narrow width of the sampling track. On the other hand, lidar missions with very high spatial coverage, like IceSat-1 or IceSat-2, have the proven potential to measure water level at very high accuracy over a large number of lakes worldwide [28] due to their long revisit times that however lead to missing subseasonal variabilities and rapid changes in lake levels.

To overcome the combined challenges of the current fleet of satellite sensors and the limitations of existing *in-situ* gauge networks, one possible solution to monitoring lake water level is the application of citizen science in monitoring waterbodies [29], [30], [31]. Citizen science is an emerging science where the public participates and collaborates in scientific research to increase knowledge. One example of the use of citizen science is the Lake Observation by Citizen Scientists and Satellites (LOCSS) (https://www.locss.org/) program, where citizen scientists report the water height elevation of lakes or wetlands by reading staff gauges [30]. Hereafter, we use the terms height and elevation interchangeably to refer essentially to the vertical dimension of lakes reported by citizen scientists to estimate volume change. The objective of the LOCSS project is to work with stakeholders and local communities, who are responsible for understanding and documenting the physical behavior of lakes or depend on lake information for decision-making activities. The purpose of

TABLE I
SUMMARY OF SENSORS AND TECHNIQUES USED FOR LAKE AREA ESTIMATION

Sensor	Revisit time	Technique	Band (wavelength, micrometers)	Threshold
L8	16 days	Dynamic surface water extent (DSWE)	Blue (0.45–0.51); Green (0.53–0.59); Red (0.64–0.67); NIR (0.85–0.88); SWIR1 (1.57–1.65); SWIR2 (2.11–2.29)	N/A
		Modified normalized difference water index (MNDWI)	Band 3–green band (0.53–0.59); band 6–short-wave infrared (1.57–1.65)	0.3
S1	10 days	Backscattering thresholding	–	< -13 dB
S2	6 days	Dynamic surface water extent (DSWE)	S2A–blue (0.496); green (0.56); red (0.664); NIR (0.835); SWIR1 (1.613); SWIR2 (2.202)	N/A
			S2B–blue (0.492); green (0.559); red (0.665); NIR (0.833); SWIR1 (1.610); SWIR2 (2.185)	

this article is to understand how different methods for estimating lake volume change combining satellite measurements of inundation extent with LOCSS measurements of water surface elevation, impact our ability to accurately detect variations in lake volume. By exploring an ensemble of methods and sensors to estimate area and consequently volume changes, we can derive a robust understanding of estimation uncertainty for lake volume changes. This understanding can be further nuanced for a given region that is unique to the season and other geophysical drivers, such as cloud cover, rainfall, topography, and water surface temperature in regions where lakes freeze.

This article explores uncertainty in volume estimation, which can provide valuable information to the decision-makers or stakeholders to make more robust decisions based on uncertainty. There are various factors that affect uncertainty in volume estimation. For example, in South Asia, a key source of uncertainty is likely to be cloud cover during monsoon for the optical sensors and inundated vegetation for SAR microwave sensors. At higher latitudes or mountainous regions where lakes freeze, the area estimation may be more challenging due to the limitations of detecting inundation variations due to ice cover or due to the shadow effect of the high topography.

In this article, we have explored four different techniques that monitor inundation extent, and thus estimate volume (Table I). The key research question being addressed is—*what is the range of uncertainty associated with estimating the volume of lakes and wetlands using current sensors, and how does this uncertainty vary as a function of geography, season, and average environmental conditions?* We used data from 94 lakes and wetlands, in which water level changes were monitored by LOCSS citizen scientists. Validation of water levels collected by citizen scientists against automated water level gauges shows that they are highly accurate, with uncertainties of less than 2 cm [30]. Such high performance in lake level estimation can be achieved only for very large lakes using satellite altimetry. We have also used data from noncitizen programs (such as automatic gauging) when necessary to fill in gaps in our lake water height database.

The structure of the article is as follows. In Section II, we discuss the study sites and datasets from the satellites and citizen science. In Section III, we discuss the methodology, and in Section IV, we discuss the result. Finally, in Section V, we discuss the implications of our results and summarize the article's conclusion.

II. DATASETS AND STUDY SITES

A. Study Sites

To better understand the complex nature of uncertainty in volume estimation and how it varies at different locations, we monitored 94 lakes and wetlands globally from the LOCSS program (Fig. 1). We focused on water bodies from the South Asian region (Bangladesh, Nepal, and India). For North America, LOCSS lake height data were obtained from water bodies located in Illinois, Massachusetts, New Hampshire, North Carolina, New York, and Washington. In Europe, we had LOCSS lake height data located in South of France in the Pyrénées mountain.

Figs. 1 and 2 show the location of the studied lakes and wetlands. The lakes in the USA and France are perennial, with some that freeze during winter. On the other hand, most of the lakes and wetlands in Bangladesh are seasonal, where water accumulates during the months of the monsoon (June to November). Readers can find supplemental information on the water body names and their exact locations from the LOCSS website (https://www.locss.org/).

B. Satellite Sensor Dataset

For estimating the surface water area, satellites missions Sentinel 1, Sentinel 2, and Landsat 8 were used. Sentinel 1 has C-band SAR imaging that can penetrate clouds and has a spatial resolution of 10 m. Revisit time of a single Sentinel

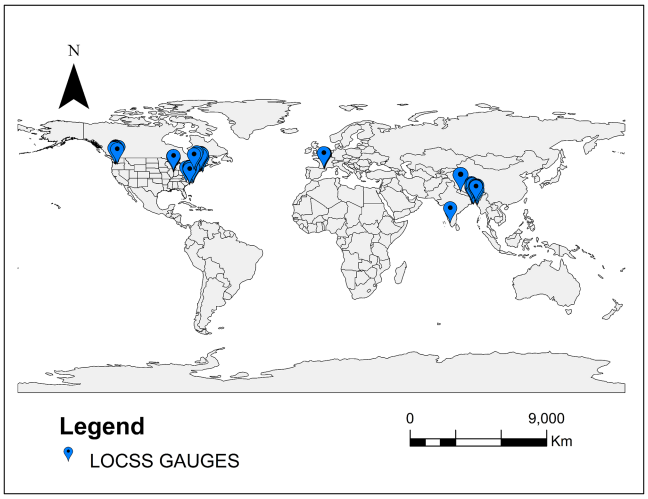

Fig. 1. Location of LOCSS sites for the citizen science monitoring of lakes and wetlands.

1 satellite is 12 days, whereas the two-satellite constellation offers a 6-day revisit time [32]. Imagery from the Sentinel 2 multispectral instrument was used with a spatial resolution of 10 m and revisit time of 5 days. Landsat 8 Operational Land Imager (OLI) Tier-1 Surface Reflectance with a spatial resolution of 30 m and revisit time of 16 days was used. These sensors were chosen as they were publicly available and have shown skill in detecting water surfaces [33], [34], [35], [36]. The satellite data are freely available on Google Earth Engine, a cloud-based computing platform ideally suited for a global study of lakes [37].

The water elevation data were collected from the citizen scientists engaged or partnered via the LOCSS program. For example, lake water height data from South Asia were obtained from citizens engaged with the relevant state or national government water agencies, such as Bangladesh Water Development Board for Bangladesh, Kerala Centre for Water Resources Development and Management for India, and Nepal Department of Hydrology and Meteorology for Nepal. Similarly, most lake height data over the USA were obtained from citizen scientists in the area with gauges were maintained by local partnering organizations. In France, the lake heights were collected by hikers who had sent photos of the gauges via smartphone. For more details, the reader is referred to [30] and www.locss.org. A previous article on LOCSS has shown the water elevation data from citizen scientists are reliable and accurate when compared to automated gauges [30]. Nevertheless, all LOCSS data were subject to a quality control to filter out human errors that represented clear outliers. A clear outlier is one where the lake water height data is found to be a random anomaly from the underlying trend observed before and after. Such outliers were replaced with a 95% percentile threshold shown in Fig. 3 below. For the case of France, the photos sent that were grainy and unreadable were discarded. The presence of such outliers occurred in less than 0.1% of the data. LOCSS gauges were installed in 2017 in the USA and France, 2019 in Bangladesh, and 2021 in Nepal.

III. Methodology

The flowchart for the methodology followed is shown in Fig. 4. The methodology has four key components as follows: 1) extracting water surface area of lakes and wetlands; 2) estimating the volume stored for all the water bodies; 3) repeating steps 1) and 2) using other methods (Table I) to create an ensemble of estimates; and 4) comparing the uncertainty in estimated volume as a function of region, nominal lake area, and geophysical factors, such as cloud cover and water surface temperature. From here onwards, we will use the terms uncertainty and uncertainty in volume estimates interchangeably.

A. Extracting Water Surface Area

1) Landsat 8: The Landsat 8 OLI/TIRS (L8) sensor was used to estimate the water surface area through a variety of water classification techniques. Atmospherically corrected L8 data using the Land Surface Reflectance Code [38] were used for the article. Two water classification techniques were used. The first was the DSWE [14]. DSWE has the ability to extract the water surface where the pixel is partially covered with vegetation and water. In addition to Landsat imagery, DSWE uses a digital elevation model, slope, hill, and cloud shade. These parameters are calculated using the Fmask function [39]. The output of the DSWE consists of six possible classes: not water, water—high confidence, water—moderate confidence, potential—wetland/partial surface water conservative, and masked out due to the cloud, cloud shadow, or snow. The second technique used to extract the water surface area is the MNDWI. Xu [12] developed the definition using the green band with short wave infrared band to detect the water feature in built-up areas where a threshold of 0.3 for the MNDWI was found to be a robust choice [40], [41]. MNDWI can be calculated using (1) below. Due to multiple equations used in the DSWE method, readers are advised to read Jones [14] for more details

$$\text{MNDWI} = \frac{\text{Green} - \text{SWIR}}{\text{Green} + \text{SWIR}}. \tag{1}$$

2) Sentinel 2: Optical imagery from Sentinel 2 (S2) sensor has a spatial resolution of 10 m, which is an improvement over the Landsat 8 spatial resolution of 30 m. The DSWE technique was also applied to Sentinel 2 images. As the DSWE algorithm was designed specifically for the L8 images, scaling of S2 reflectance data is required to make DSWE work for S2 data. Surface reflectance transformation functions between S2 and L8 can be used to transform the S2 bands to L8 bands. In the article, we used the transformation function developed by Zhang et al. [41] to linearly map the S2 bands to L8 bands and use the DSWE algorithm. For the MNDWI technique on S2 imagery, no transformation is required according to the study conducted by Du et al. [42].

3) Sentinel 1: Sentinel 1 is an angle looking C-band SAR that sends radar signals which can penetrate clouds. Water classification using the Sentinel 1 imageries was accomplished with the help of the backscattering thresholding technique. Nonwater surfaces usually have high roughness and thus, they have high backscattered energy as compared to the water-like surface.

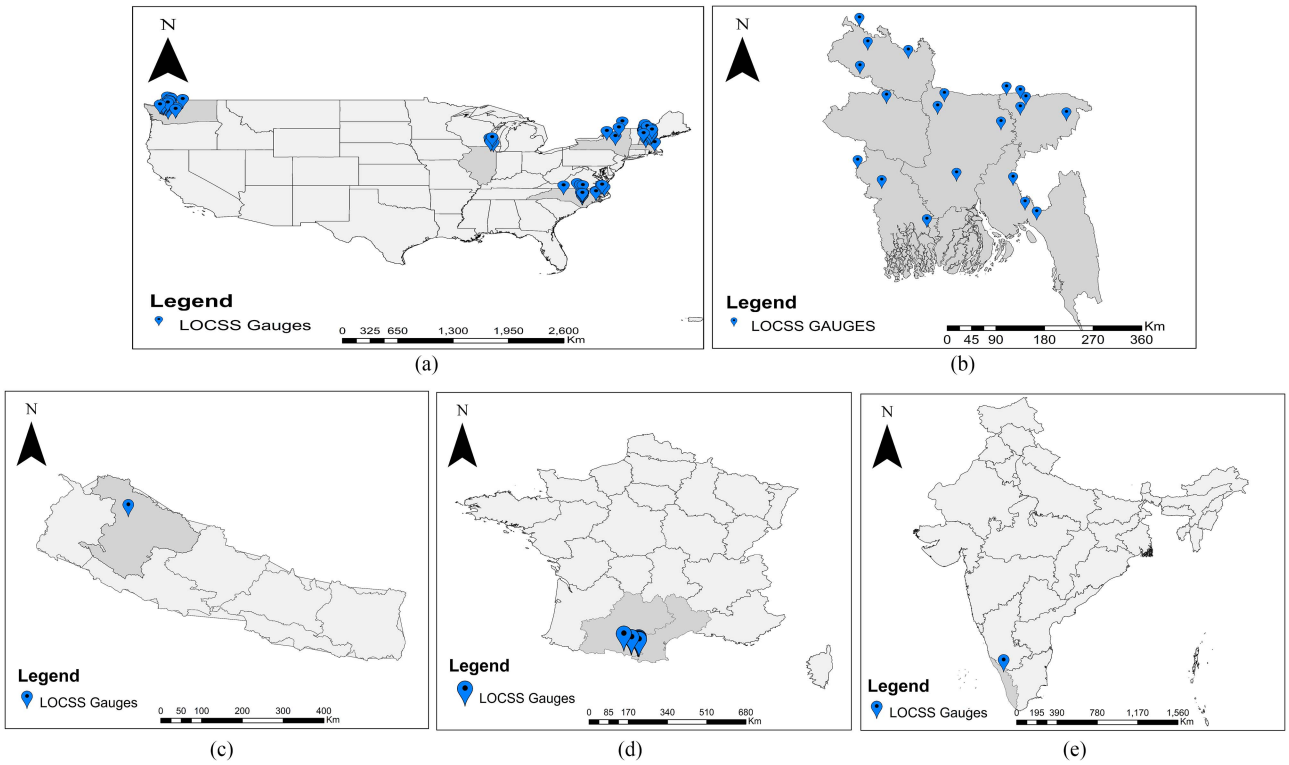

Fig. 2. Location of LOCSS gauges in (a) USA (59 lakes), (b) Bangladesh (20 lakes), (c) Nepal (1 lake), (d) France (13 lakes), and (e) India (1 lake).

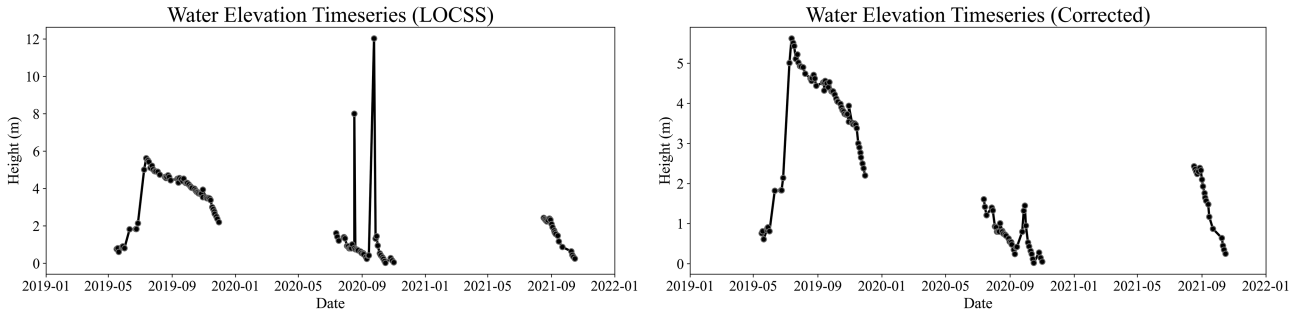

Fig. 3. Example of water surface elevation before and after correction of outliers.

The water-like surfaces appear dark in the imagery because of their smooth surface. Hence, this phenomenon can be used to extract the water surface extent by putting a threshold on the backscatter values. However, one of the drawbacks of the SAR is speckle noise, which degrades the quality of the image and causes information loss. Over the years, various techniques have been used to reduce the speckle noise, such as wavelet transform [43] and mean–median filters [44]. We used a focal median filter with a 30 m $\times$ 30 m window. Incidence angle also plays an important role in the image preprocessing; for the water surface classification, we considered look angles from 31.7° to 45.4°. More details on this choice are described by Ahmad et al. [29]. With the preprocessed image, a backscatter threshold of -13 db was selected to identify the water body, as suggested by Liu [45].

B. *Extracting Water Surface Elevation*

The water surface elevations were gathered with the help of citizen scientists. The data for all the water bodies were downloaded from the LOCSS website where they are publicly available.

C. *Estimating the Volume Stored and Generating Uncertainty Ensemble*

After estimating the water surface area and extracting the water surface elevation, volume of water stored above the minimum observed level was estimated for each of the techniques and sensors. Satellite water extent data were used for days that matched or were within 3 days of the measurement date of citizen scientists from LOCSS. To estimate the volume variation,

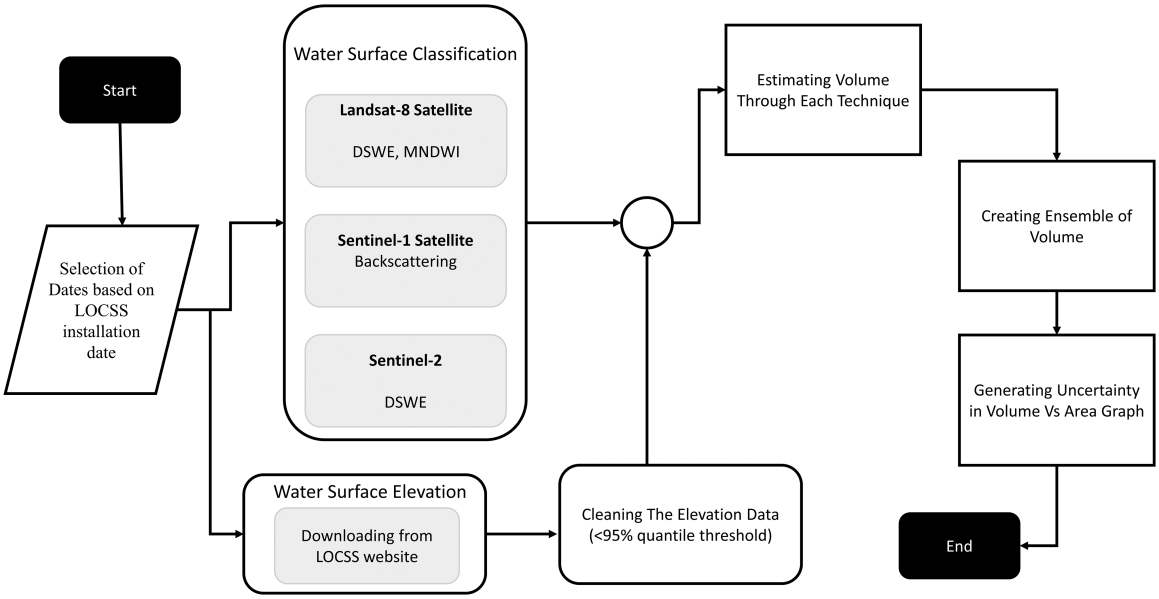

Fig. 4. Flowchart for methodology used for exploring uncertainty of satellite-based lake volume estimation.

we linearly interpolated the water surface area data, so that the timestamps of both water elevation and interpolated water surface area were the same, which makes it easier to calculate the volume change. The information of the exact bathymetry of the water bodies was not available, so we estimated the volume stored with respect to the lowest observed water surface elevation in the time series, similar to Ahmad et al. [29] who had earlier applied citizen scientist height data for northeastern wetlands of Bangladesh. The lowest water elevation observation was obtained from the LOCSS website over the period of the study. For simplicity, many articles in the past have assumed trapezoidal bathymetry [29], [30], so we also assumed trapezoidal bathymetry. Pyramidal bathymetry of lakes can also be assumed as proposed in Cretaux et al. [26] but internal comparison done between both hypotheses have usually yielded very similar results. Hence, volume stored by the water body at a given time can be calculated as

$$V_t = \frac{(h_t - h_{\min})\,(A_t + A_{\min})}{2}\,[L3]\,. \tag{2}$$

Here, in (2), h_t is the water elevation at time t and $h_{\min}$ is the lowest water elevation of the time series at each lake. A_t is the area of the lake at time t and $A_{\min}$ is the minimum area of the lake. The volume estimated in this fashion using (2) yields the volume that can be estimated from the lowest level observed in the satellite record. Understandably, this approach may yield large errors when the difference between h_t and $h_{\min}$ is large enough to disqualify the assumption of trapezoidal bathymetry between those two heights. In our scrutiny of bathymetries above the minimum observed level, lakes that experience large height difference of many meters, such as in Bangladesh (South Asia), follow a very flat and steady trapezoidal bathymetry. In regions where bathymetry shape may be irregular over large heights, such as in the studied lakes of Europe, USA, India, and Nepal, the height differences reported by citizens are usually not large enough.

The volume stored was estimated for all four techniques used in the article (Table I), and an ensemble of the volume estimates was generated. Fig. 5 shows an example of the ensemble of estimated volumes.

D. Studied Factors Affecting Uncertainty

1) South Asia: To understand the complexity of uncertainty in estimating volume, various factors contributing to the uncertainty were studied. Countries, such as Bangladesh, India, and Nepal, have a monsoonal climate, which brings extensive cloud cover and a high amount of rainfall for 3–5 months. Hence, precipitation patterns and cloud cover were compared with uncertainty. Optical sensors have a limitation that they cannot penetrate the clouds. The complementary nature of optical and radar sensors with unique strengths and weaknesses collectively give rise to estimation uncertainty. Gridded precipitation data for Bangladesh were downloaded from the ERA5 hourly precipitation and gridded precipitation data for India were downloaded from Indian Meteorological Department. The cloud cover data were collected from information provided in the Landsat 8 satellite data product. Table II shows the information about the dataset used.

2) North America: In the regions of North America studied here, the monsoon is not as dominant, unlike South Asia. We therefore studied the uncertainty in volume estimation as a function of temperature and cloud cover. The water surface temperature of lakes was estimated using the Landsat 7 Collection 1 Tier 1 (L7). Low-gain Thermal Infrared 1 Band (B6_VCID_1)

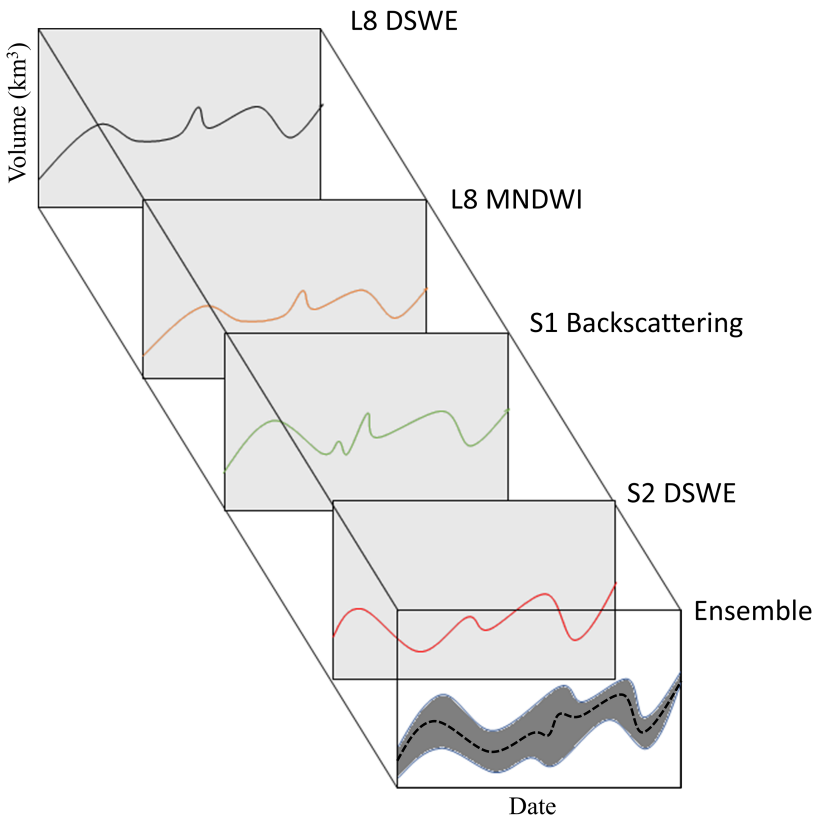

Fig. 5. Schematic showing how ensemble and range of estimates on volume change are generated using different methods and sensors.

TABLE II
ADDITIONAL INFORMATION ON THE DATASET USED IN THE STUDY

Dataset	Downloaded from	Spatial resolution
Sentinel 1 (S1)	Data ID on Google Earth Engine: ee.ImageCollection("COPERNICUS/S1_GRD")	10 m
Sentinel 2 (S2)	Data ID on Google Earth Engine: ee.ImageCollection("COPERNICUS/S2_SR")	10 m
Landsat 8 (L8)	Data ID on Google Earth Engine: ee.ImageCollection("LANDSAT/LC08/C01/T1_SR")	30 m
Precipitation (Bangladesh)	https://cds.climate.copernicus.eu/cdsapp#!/dataset/reanalysis-era5-land?tab=form	0.25° grid
Precipitation (India)	https://www.imdpune.gov.in/cmpg/Griddata/Rainfall_25_Bin.html	0.25° grid
Temperature	Derived from Landsat 8 Thermal Infrared Band	60 m

was used to estimate the temperature, while the cloud cover over the water bodies was estimated using L8.

3) Europe: In Europe, we studied the water bodies in France. All of the lakes in France were in highly mountainous areas of the Pyrenees. Thus, with the exception of Nepal, these lakes were located in the most topographically variable landscape of any LOCSS lakes. These lakes also freeze in the winter. We ran the same analysis on France as we did on North America.

E. Estimating the Uncertainty in Volume Estimation

We chose a metric for uncertainty in volume estimation that provides us with an idea for average spread of the estimated volumes over time relative to the statistically expected volume of a water body (also over time). Here, the expected volume is assumed to be the arithmetic mean of the volumes estimated by the four methods. We call this metric the "time-averaged uncertainty." This time-averaged uncertainty metric is calculated using (3). Here, we use the time-averaged uncertainty metric in relative terms normalized by the mean volume to allow comparison across all lakes and regions. A time-averaged uncertainty metric value of less than 1 means that the current suite of satellite sensors and methods is generally able to estimate volume variations with a spread that is less than the mean value, and hence the uncertainty may be considered acceptable most times. Vice versa, an uncertainty metric value of more than 1 means the spread of uncertainty is significantly larger than the mean value itself, and hence the volume uncertainty may be

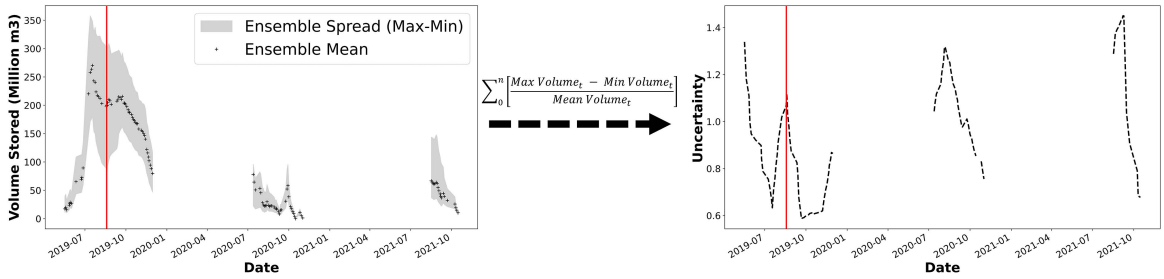

Fig. 6. Volume stored and uncertainty time-series for Korchar wetland in Bangladesh.

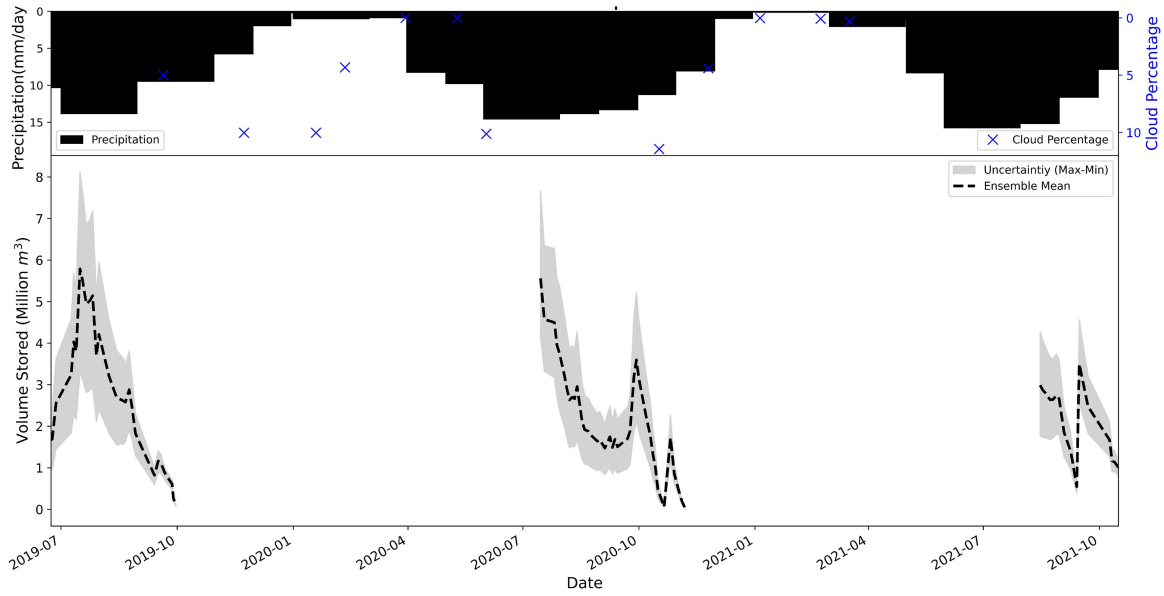

Fig. 7. Time-series of uncertainty of volume estimation of Dekhar Haor wetland in Bangladesh.

considered unacceptable. Fig. 6 illustrates how the time-specific uncertainty in the volume varies for the Korchar wetland in Bangladesh over time to yield the time-averaged uncertainty metric defined in (3).

The time-specific behavior of uncertainty is particularly suited for developing a temporal understanding of seasonal water bodies, such as wetlands in South Asia. During the development of a wetland in the monsoon season, the spread of the ensemble may be smaller yet the uncertainty metric for that specific time can be higher because of time-specific low mean for estimate volumes. Such a high time-specific uncertainty can be indicative of the limitation of the sensors for water bodies with very small volumes and variations at that time. As these wetlands develop and the volume stored increases, the time-specific uncertainty metric can decrease if the collective precision of the sensors holds. Conversely, the opposite can happen with time-specific uncertainty rising as volume increases. We show one such example in Fig. 6(a) and (b). A red line is shown to demonstrate the case for a wetland in Bangladesh where the time-specific uncertainty rises despite increase in volume after the height of the monsoon in August. This corroborates the fact that uncertainty of volume estimation can be dependent on many factors, many of which are time-specific (such as cloud cover, land temperature, growth of vegetation, and irregular/nontrapezoidal bathymetry)

$$\text{Time averaged Uncertainty} = \frac{\sum_0^n \left[\frac{\text{Max Volume}_t - \text{MinVolume}_t}{\text{MeanVolume}_t}\right]}{\sum_0^n t}. \tag{3}$$

IV. Results

In this section, we demonstrate a few examples of time-varying uncertainty (not the time-averaged uncertainty) that are representative of lakes and wetlands for their regions. Fig. 7 shows the volume estimation uncertainty of a wetland in Bangladesh. In general, the wetlands in Bangladesh are fully inundated during May–December, while from January to April, they are often dry. It is seen that during higher cloud cover and precipitation, the uncertainty spread is high. Fig. 8 shows the ensemble of Pookode lake in Kerala, India. Kerala in general receives two monsoons. One is the southwest monsoon (June–September) and the other is the northeast monsoon (October–December). Essentially, the entire period of June–December is characterized by extensive cloud cover. We observe that volume stored and uncertainty in volume are both higher as the monsoons retreat in December with gradual decrease as cloud

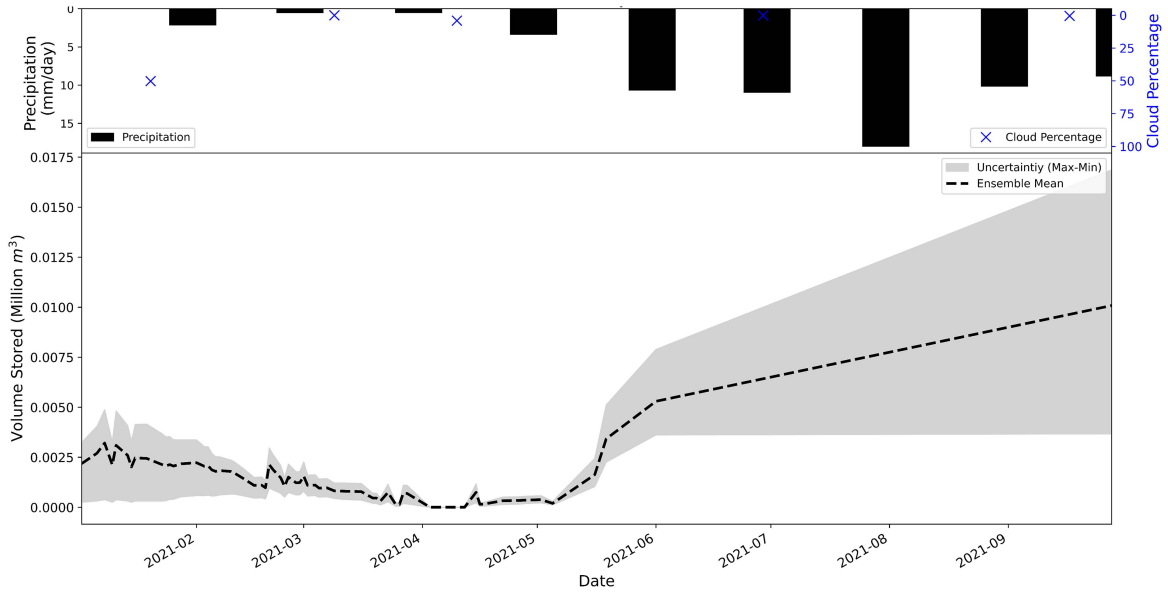

Fig. 8. Time-series of uncertainty of volume estimation in Pookode lake in Kerala (India).

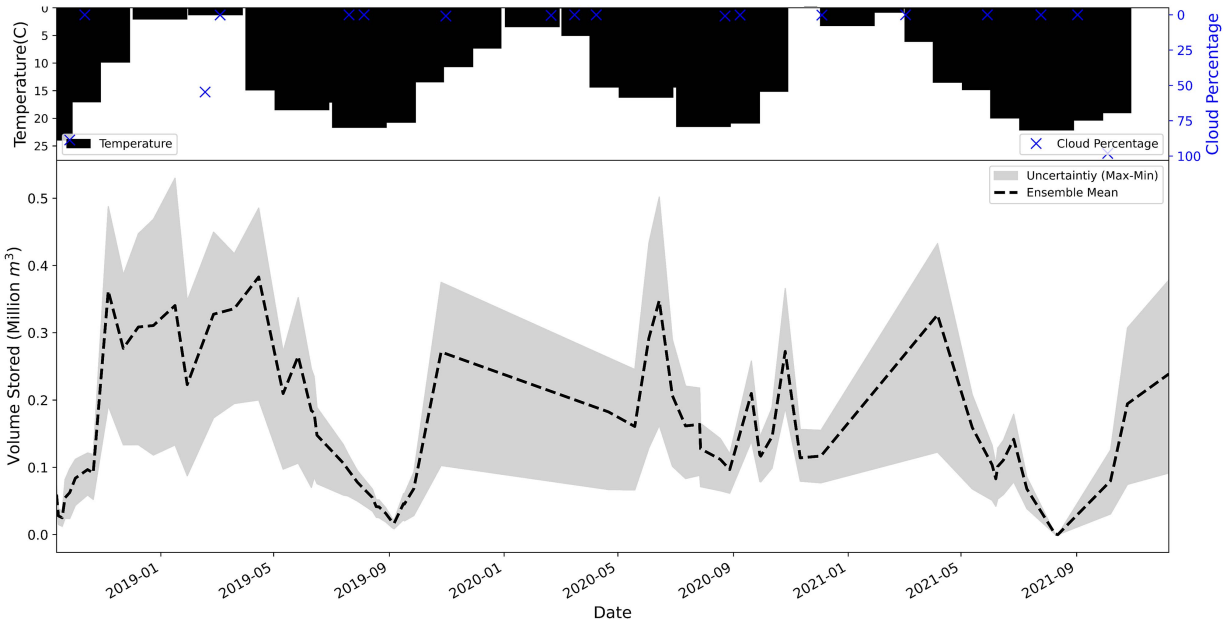

Fig. 9. Ensemble of volume change estimates by different methods and sensors for Cassidy lake in Washington state (USA). Note: here, *y*-axis represents volume change rather than volume.

cover and precipitation decreases in April. The pattern repeats itself from June to December again as the two monsoon seasons complete their cycle.

For U.S. lakes, we studied volume uncertainty as a function of cloud cover and water surface temperature, given the tendency of some lakes in upper latitudes to freeze during winter. In Figs. 9 and 10, we show the uncertainty spread for Cassidy Lake (Washington State) and Rara Lake (Nepal), which is found to be high during freezing conditions. When volume stored is low, the uncertainty spread is also found to be quite high. As there are likely many other controlling factors, water temperature provides only a partial explanation of the temporal behavior of uncertainty.

To estimate the benchmark volume change, we used higher spatial resolution dataset from Planet at 3 m [48]. The assumption we make here is that a significantly higher spatial resolution visible dataset during clear sky conditions should be able to capture areal extent and hence volume changes much more accurately and precisely than the satellite sensors used in this article at coarser spatial resolution. We understand this

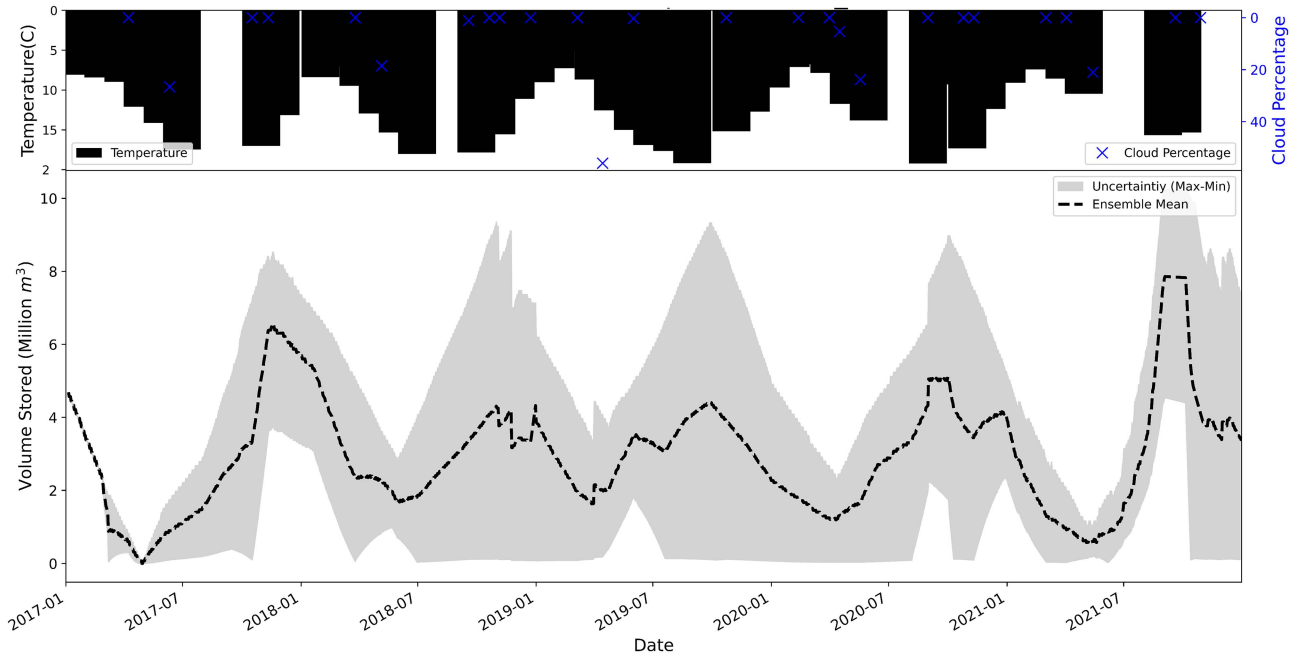

Fig. 10. Ensemble volume change estimates by different methods and sensors for Rara lake in Nepal. Note: here, *y*-axis represents volume change rather than volume.

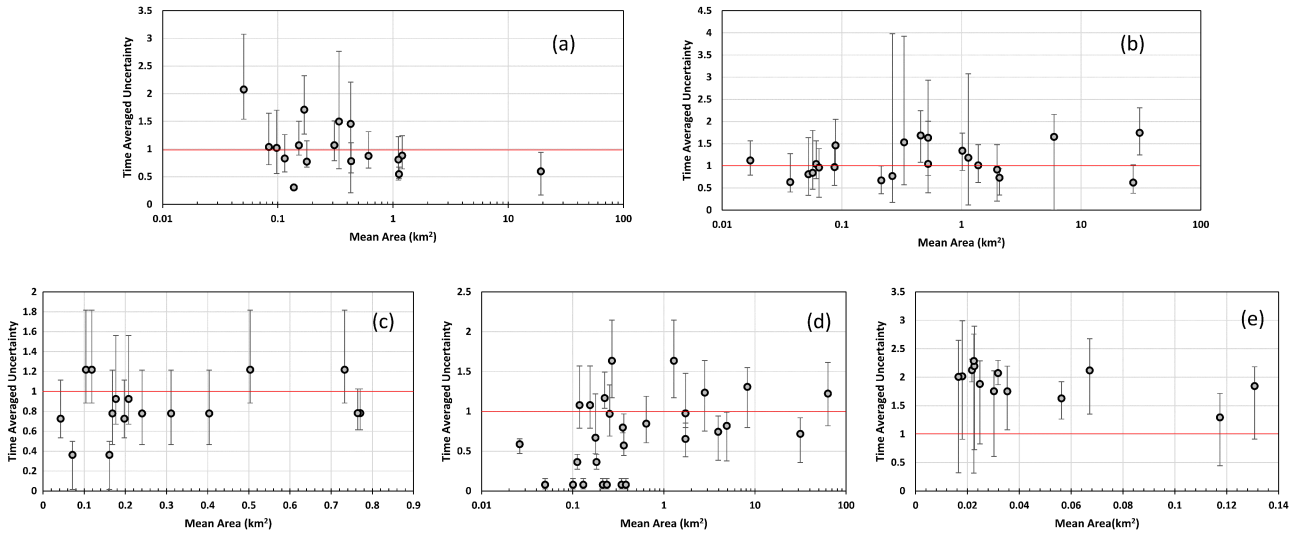

Fig. 11. Time-averaged uncertainty metric in volume vs. nominal lake area for (a) Washington (USA), (b) Bangladesh, India, and Nepal, (c) Illinois, (d) New York, Massachusetts, North Carolina, and New Hampshire, (e) France. Lakes below the red line are assumed to yield acceptable uncertainty using the threshold value of 1.

assumption may not always hold as there are other factors related to the bathymetry, color of water, and surrounding background region that can also play a compounding role regardless of sensor's spatial resolution. Nevertheless, we believe that use of 3-m Planet data is worthwhile as it provides an "alternative" to readers to help them grasp the nature of uncertainty they may expect in using the coarser resolution satellite data of S1, S2, and Landsat. Table III shows the extent of the water bodies as well as their benchmark volume (second column from left). We estimated the volume at the time when volume of water stored is maximum and minimum. We found that our ensemble mean was close to the benchmark volume and the range of ensemble volumes clearly encapsulates the benchmark volume.

Fig. 11 shows the time-averaged uncertainty metric (3) for all the water bodies as a function of the nominal lake area. Fig. 11 is a plot showing the aggregate behavior volume estimation uncertainty for each region as lake area changes. Fig. 12 shows the same but for areal estimation uncertainty for each region as nominal lake area changes. The idea is to understand if there is a threshold area for a lake size below which the time-averaged

TABLE III
BENCHMARK VOLUME CHANGE OF SELECTED WATER BODIES USING HIGHER RESOLUTION DATA IN COMPARISON TO SATELLITE-BASED METHODS

Benchmark lake image Blue: water; Green: nonwater	**Name (month)**	**Benchmark volume change (million m^3)**	**Ensemble mean of volume change (million m^3)**	**Ensemble range of volume change (million m^3)**
	**DEKHAR** (BANGLADESH) (JULY)	5.856608	4.497891	6.28–3.17
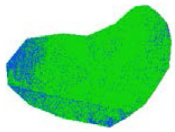	**DEKHAR** (BANGLADESH) (NOVEMBER)	0.113676	0.197754	0.24–0.15
	**KORCHAR** (BANGLADESH) (JULY)	265.543071	272.620922	334.54–215.68
	**KORCHAR** (BANGLADESH) (OCTOBER)	10.965009	13.986204	19.80–9.17
	**SAMMAMISH** (USA) (JANUARY)	11.221755	9.247892	13.26–4.49

uncertainty metric is unacceptable (>1). From Figs. 11 and 12, the percentage of water bodies having uncertainty metric less than or equal to 1 in Washington, South East Asia (Bangladesh, India, and Nepal), Illinois, and East Coast USA (New York, Massachusetts, North Carolina, and New Hampshire) is found to be 75%, 55%, 75%, and 71%, respectively. These numbers are believed to be statistically robust according to our tests of significance using the student *t*-test. Using the student *t*-test, we found within the 95% confidence interval, the mean time-averaged uncertainty metric of lakes in South Asia to be 1.11 (±0.16). Similarly, for lakes in the USA, the mean uncertainty metric is 0.71 (±0.184) at the 95% confidence interval. What is evident from our tests of significance is that the results we have derived for time-averaged uncertainty are significant as the variability (shown within parentheses) is an order lower than the mean estimate in the 95% confidence interval based on the student *t*-test.

To understand the role played by individual area estimation methods in volume estimation uncertainty, we ranked each of the four methods from highest to lowest average volume estimates for a give lake. In Fig. 13, we show in a four panel plot the methods for each lake with highest estimate (upper most

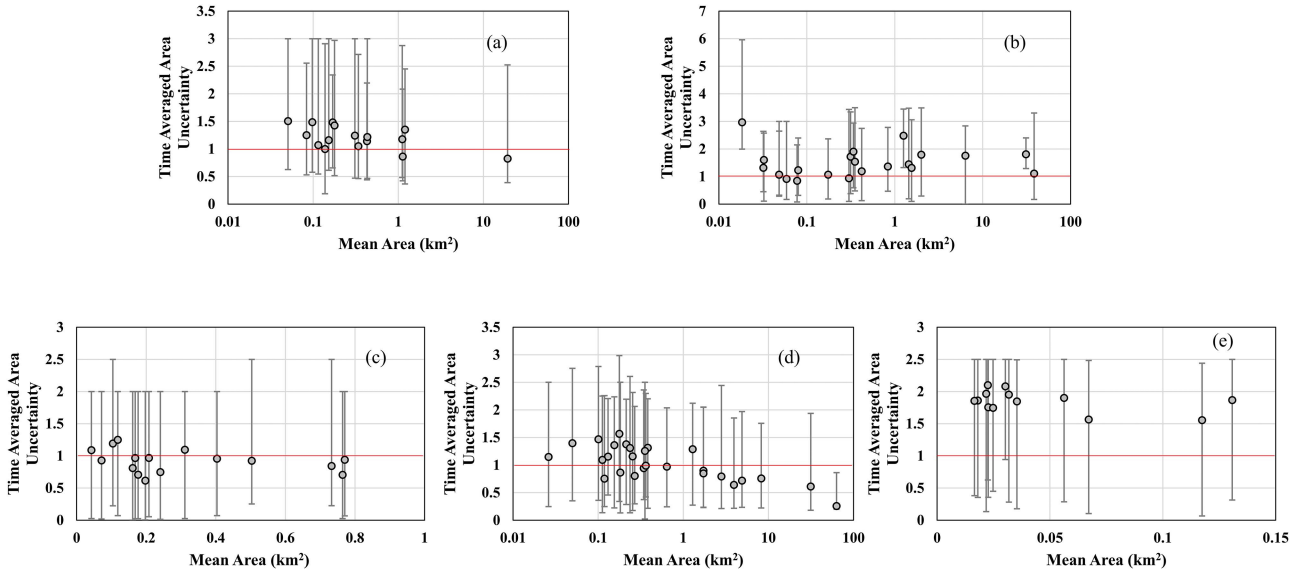

Fig. 12. Time-averaged uncertainty metric in areal extent vs. nominal lake area for (a) Washington (USA), (b) Bangladesh, India, and Nepal, (c) Illinois, (d) New York, Massachusetts, North Carolina, and New Hampshire, (e) France. Lakes below the red line are assumed to yield acceptable uncertainty using the threshold value of 1.

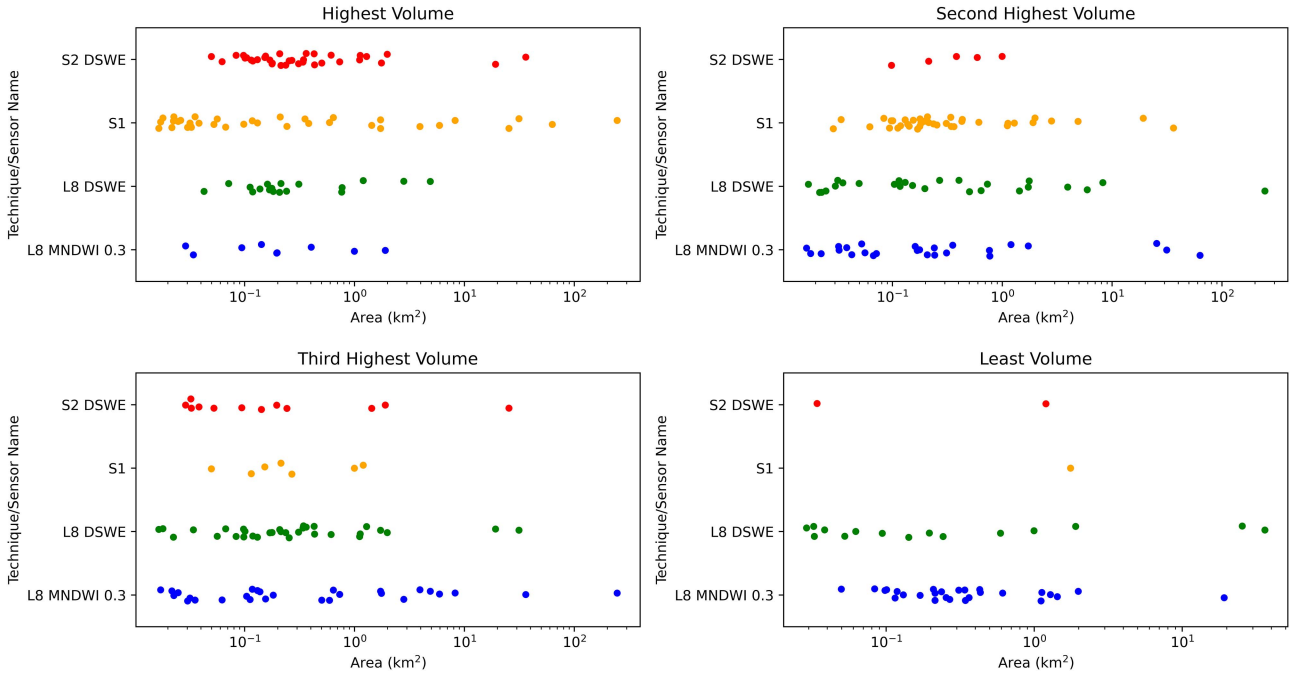

Fig. 13. Ranking of the four methods shown as a function of nominal lake area on *x*-axis. A unique color is assigned to each of the four techniques/sensor. Each dot represents a particular lake and a particular method applied for volume change analyses. Each panel shows how many times a particular technique/sensor, as defined by its unique color, produces the highest (upper left), second highest (upper right), third highest (lower left), and least (lower right) volume change estimate. The entire ensemble of studied lakes for a given technique/sensor is represented by the total number of dots pertaining to the specific color across all panels, or the total number of dots in a given panel. The panels collectively show that no particular method is biased in over or underestimating from the mean of the ensemble.

panel), second-highest estimate (middle panel), second-lowest estimate (second panel from bottom), and lowest estimate of volume (bottom most panel). The idea is to see if performance of methods is consistent across lakes or if other geophysical factors pertaining to the lake and the ambient environment control the tendency to estimate the highest or lowest value of the ensemble. In general, the DSWE method using Sentinel-2 and Sentinel-1 based backscattering method have a tendency to yield higher volume estimates. However, when looked as a whole, there does not seem to be single method that is found to consistently estimate the highest, lowest volume, or median volume. This indicates that in this article of lake volume estimation uncertainty, there is no single method that can be filtered out to minimize uncertainty and that all methods should be considered collectively to improve our understanding of uncertainty.

V. Discussion and Conclusion

We studied 94 lakes and wetlands around the world where LOCSS gauges were installed to record water elevations measured by citizen scientists. We defined time-averaged uncertainty metric and used a value of 1 as the cutoff for acceptable uncertainty (<1) or unacceptable uncertainty (>1). When looked as a whole for all the lakes studied, there is no clear pattern in our findings where lakes larger than a certain threshold can claim to experience higher skill in estimation of volume. However, at individual regions, there are some nuanced patterns. For example, lakes in Washington (Fig. 11, panel a) and France (Fig. 11, panel e) show a clear dependency of uncertainty as a function of area where the time-averaged uncertainty metric decreases as nominal lake area increases. In South Asia, lakes larger than 0.05 km^2 (mostly in Bangladesh; Fig. 11, panel b) experience an uncertainty metric of less than 1 in 75% of cases without a clear dependency on lake area. This implies that the flat terrain nature of Bangladesh topography combined with more dynamic hydrometeorological and land use patterns compared to other regions studied pose significant challenge to lake volume estimation. In the USA, lakes east of the 108th meridian (Colorado Rockies) exhibit considerably lower uncertainty in volume estimation compared to the Pacific Northwestern region of Washington (compare panels a, c, and d in Fig. 11). This uncertainty decreases gradually for lakes located further eastwards, starting from Illinois to Eastern USA (Massachusetts, New York, North Carolina, and New Hampshire). For example, in Washington state, the average time-averaged uncertainty appears to be around 20% higher than lakes in Illinois which are about 50% higher than lakes in the eastern USA. It is clear that much smaller sized lakes in the eastern USA can be estimated with considerably less uncertainty. In France, we observe that the spread of the uncertainty is consistently high and exceeding the threshold value of 1. One of the plausible reasons for this can be the shadow of the mountains. The LOCSS gauges are installed in south of France, near the Pyrenees mountains. While digitizing the lakes in France, mountains projecting a shadow on water bodies were observed. Ji et al. [46] discussed how mountain shadows can be misclassified as water pixels. We should however exercise caution in interpreting the volume estimation uncertainty pattern for each region (e.g., USA, France, and South Asia) given that sample of lakes studied here are not necessarily a statistically large sample to represent all the regions.

Our lake height data were obtained from the citizen science program of LOCSS, which has the additional objective of validating and improving lake products anticipated from the recently launched Surface Water and Ocean Topography (SWOT) mission. The SWOT satellite mission is a joint mission of the NASA and Centre National d'Etudes Spatiales (CNES) with contributions from the Canada Space Agency and the United Kingdom Space Agency. SWOT is planned for launch in November 2022 [47]. It will be the first satellite of its kind that will report water surface elevation and water surface area simultaneously with a revisit time of 21 days or less at a given location. The primary instrument on SWOT is Ka-band Radar Interferometer, which uses radar interferometry and SAR, which gives high-resolution water elevation and inundation extent [47]. Currently, as noted in this article, to estimate the volume, water surface area is derived from satellite sensors while the elevations are obtained either from concurrently flying altimeters or from the *in-situ* data. SWOT, with its simultaneous measurement of area and elevation, will improve our ability to estimate volume more consistently. Moreover, SWOT is a swath interferometer which will cover the whole Earth and monitor lakes larger than 250×250 m. This will be an unprecedent view of the lake storage change dynamics at the global scale.

Our findings therefore have implications for the SWOT mission. First of all, the availability of LOCSS gauge data from citizens can be expected to provide valuable validation data to compare SWOT-estimated volume changes once SWOT starts to provide lake area and elevation simultaneously. Second, SWOT observables could be combined with pre-SWOT satellite data to create higher frequency estimates of lake volume with lower estimation uncertainty. Armed with a general idea of what regions, specific factors and the minimum lake size matter in achieving an acceptable uncertainty, LOCSS gauges can be strategically expanded or the data quality for lake storage change can be flagged accordingly.

The estimation of uncertainty for volume is also useful for practical applications at ungauged regions lacking historical records, such as sizing of surface water storage facilities or flood control structures. For example, if an urban settlement is planned in the ungauged region with no historical records, where lakes are the only source of surface water, then the freshwater storage and distribution system size would need to be based on the minimum (worst case) scenario of lake volume experienced over a sufficiently long period. Similarly, a flood protection facility in the same ungauged region would have to be designed based on the maximum (worst case) scenario of lake volume observed over a long record. The range of estimation uncertainty gleaned from an ensemble of satellite sensors and techniques facilitates such societally relevant application in the design of water management facilities at regions lacking historical *in-situ* records. In a previous effort based on LOCSS [29], the estimation of total volume stored in northeastern Bangladesh with uncertainty has already triggered a conversation by the Bangladesh Government to exploit any excess surface water for commercial revenue-generating purposes (personal communication with Director General of Bangladesh Water Development Board).

This article is not without limitations. One key limitation is the short period of LOCSS data for many regions, such as South Asia. Lack of *in-situ* three-dimensional bathymetry over time to capture the nonstationarity due to sand deposition or transport can also be an issue. An accurate bathymetry of the lakes can also help in constraining our estimates further. We hope these limitations can be addressed in a future article as the LOCSS data continue to grow with more participation from citizen scientists around the world.

Acknowledgment

First author Khan and corresponding author Hossain were supported via a subaward from UNC. Additional support from partnering agencies is gratefully acknowledged for maintenance

of the LOCSS gauge network. These agencies are Bangladesh Water Development Board, Nepal Department of Hydrology and Meteorology, Pakistan Council of Research in Water Resources, Centre for Water Resources Development and Management-Kerala, and many state and local agencies of the USA and France.

REFERENCES

[1] M. Courouble, N. Davidson, and L. Dinesen, "Global wetland outlook special edition 2021," Secretariat of the Convention on Wetlands 2021, 2021.

[2] J. Downing et al., "The global abundance and size distribution of lakes, ponds, and impoundments," *Limnol. Oceanogr.*, vol. 51, pp. 2388–2397, Sep. 2006, doi: 10.4319/lo.2006.51.5.2388.

[3] C. Verpoorter, T. Kutser, D. A. Seekell, and L. J. Tranvik, "A global inventory of lakes based on high-resolution satellite imagery," *Geophys. Res. Lett.*, vol. 41, no. 18, pp. 6396–6402, 2014, doi: 10.1002/2014GL060641.

[4] B. Lehner and P. Döll, "Development and validation of a global database of lakes, reservoirs and wetlands," *J. Hydrol.*, vol. 296, no. 1, pp. 1–22, Aug. 2004, doi: 10.1016/j.jhydrol.2004.03.028.

[5] M. L. Messager, B. Lehner, G. Grill, I. Nedeva, and O. Schmitt, "Estimating the volume and age of water stored in global lakes using a geo-statistical approach," *Nature Commun.*, vol. 7, no. 1, Dec. 2016, Art. no. 13603, doi: 10.1038/ncomms13603.

[6] Y. Sheng et al., "Representative lake water extent mapping at continental scales using multi-temporal Landsat-8 imagery," *Remote Sens. Environ.*, vol. 185, pp. 129–141, Nov. 2016, doi: 10.1016/j.rse.2015.12.041.

[7] S. Hu, Z. Niu, Y. Chen, L. Li, and H. Zhang, "Global wetlands: Potential distribution, wetland loss, and status," *Sci. Total Environ.*, vol. 586, pp. 319–327, May 2017, doi: 10.1016/j.scitotenv.2017.02.001.

[8] D. E. Alsdorf and D. P. Lettenmaier, "Tracking fresh water from space," *Science*, vol. 301, pp. 1491–1494, Sep. 2003, doi: 10.1126/science.1089802.

[9] D. P. Lettenmaier, D. Alsdorf, J. Dozier, G. J. Huffman, M. Pan, and E. F. Wood, "Inroads of remote sensing into hydrologic science during the WRR era," *Water Resour. Res.*, vol. 51, no. 9, pp. 7309–7342, 2015, doi: 10.1002/2015WR017616.

[10] I. M. McCullough, C. S. Loftin, and S. A. Sader, "High-frequency remote monitoring of large lakes with MODIS 500m imagery," *Remote Sens. Environ.*, vol. 124, pp. 234–241, Sep. 2012, doi: 10.1016/j.rse.2012.05.018.

[11] S. K. Ahmad, F. Hossain, H. Eldardiry, and T. M. Pavelsky, "A fusion approach for water area classification using visible, near infrared and synthetic aperture radar for South Asian conditions," *IEEE Trans. Geosci. Remote Sens.*, vol. 58, no. 4, pp. 2471–2480, Apr. 2020, doi: 10.1109/TGRS.2019.2950705.

[12] H. Xu, "Modification of normalised difference water index (NDWI) to enhance open water features in remotely sensed imagery," *Int. J. Remote Sens.*, vol. 27, no. 14, pp. 3025–3033, Jul. 2006, doi: 10.1080/01431160600589179.

[13] S. K. McFeeters, "The use of the normalized difference water index (NDWI) in the delineation of open water features," *Int. J. Remote Sens.*, vol. 17, no. 7, pp. 1425–1432, May 1996, doi: 10.1080/01431169608948714.

[14] J. W. Jones, "Improved automated detection of subpixel-scale inundation—Revised dynamic surface water extent (DSWE) partial surface water tests," *Remote Sens.*, vol. 11, no. 4, Jan. 2019, Art. no. 374, doi: 10.3390/rs11040374.

[15] T. D. Acharya, D. H. Lee, I. T. Yang, and J. K. Lee, "Identification of water bodies in a landsat 8 OLI image using a J48 decision tree," *Sensors*, vol. 16, no. 7, Jul. 2016, Art. no. 1075, doi: 10.3390/s16071075.

[16] P. S. Frazier and K. J. Page, "Water body detection and delineation with landsat TM data," *Photogramm. Eng. Remote Sens.*, vol. 66, pp. 1461–1467, Jan. 2000.

[17] R. Brakenridge and E. Anderson, "MODIS-based flood detection, mapping and measurement: The potential for operational hydrological applications," in *Proc. Transboundary Floods: Reducing Risks Through Flood Manage.*, 2006, pp. 1–12, doi: 10.1007/1-4020-4902-1_1.

[18] C. Huang, Y. Chen, J. Wu, L. Li, and R. Liu, "An evaluation of suomi NPP-VIIRS data for surface water detection," *Remote Sens. Lett.*, vol. 6, no. 2, pp. 155–164, Feb. 2015, doi: 10.1080/2150704X.2015.1017664.

[19] J. Liang and D. Liu, "A local thresholding approach to flood water delineation using Sentinel-1 Sar imagery," *ISPRS J. Photogramm. Remote Sens.*, vol. 159, pp. 53–62, Jan. 2020, doi: 10.1016/j.isprsjprs.2019.10.017.

[20] X. Shen, D. Wang, K. Mao, E. Anagnostou, and Y. Hong, "Inundation extent mapping by synthetic aperture radar: A review," *Remote Sens.*, vol. 11, no. 7, Jan. 2019, Art. no. 879, doi: 10.3390/rs11070879.

[21] S. Mayr, I. Klein, M. Rutzinger, and C. Kuenzer, "Determining temporal uncertainty of a global inland surface water time series," *Remote Sens.*, vol. 13, no. 17, Jan. 2021, Art. no. 3454, doi: 10.3390/rs13173454.

[22] A. H. Pickens et al., "Global seasonal dynamics of inland open water and ice," *Remote Sens. Environ.*, vol. 272, Apr. 2022, Art. no. 112963, doi: 10.1016/j.rse.2022.112963.

[23] J.-F. Crétaux and C. Birkett, "Lake studies from satellite radar altimetry," *Comptes Rendus Geosci.*, vol. 338, no. 14, pp. 1098–1112, Nov. 2006, doi: 10.1016/j.crte.2006.08.002.

[24] F. Baup, F. Frappart, and J. Maubant, "Combining high-resolution satellite images and altimetry to estimate the volume of small lakes," *Hydrol. Earth Syst. Sci.*, vol. 18, no. 5, pp. 2007–2020, May 2014, doi: 10.5194/hess-18-2007-2014.

[25] Z. Duan and W. G. M. Bastiaanssen, "Estimating water volume variations in lakes and reservoirs from four operational satellite altimetry databases and satellite imagery data," *Remote Sens. Environ.*, vol. 134, pp. 403–416, Jul. 2013, doi: 10.1016/j.rse.2013.03.010.

[26] J.-F. Crétaux et al., "Lake volume monitoring from space," *Surv. Geophys.*, vol. 37, no. 2, pp. 269–305, Mar. 2016, doi: 10.1007/s10712-016-9362-6.

[27] J.-F. Crétaux et al., "Absolute calibration or validation of the altimeters on the Sentinel-3A and the Jason-3 over Lake Issykkul (Kyrgyzstan)," *Remote Sens.*, vol. 10, no. 11, Nov. 2018, Art. no. 1679, doi: 10.3390/rs10111679.

[28] S. W. Cooley, J. C. Ryan, and L. C. Smith, "Human alteration of global surface water storage variability," *Nature*, vol. 591, no. 7848, pp. 78–81, Mar. 2021, doi: 10.1038/s41586-021-03262-3.

[29] S. K. Ahmad et al., "Understanding volumetric water storage in monsoonal wetlands of Northeastern Bangladesh," *Water Resour. Res.*, vol. 56, no. 12, 2020, Art. no. e2020WR027989, doi: 10.1029/2020WR027989.

[30] S. Little et al., "Monitoring variations in lake water storage with satellite imagery and citizen science," *Water*, vol. 13, no. 7, Jan. 2021, Art. no. 949, doi: 10.3390/w13070949.

[31] C. S. Lowry and M. N. Fienen, "Crowdhydrology: Crowdsourcing hydrologic data and engaging citizen scientists," *Ground Water*, vol. 51, no. 1, pp. 151–156, Feb. 2013, doi: 10.1111/j.1745-6584.2012.00956.x.

[32] M. Schlund and S. Erasmi, "Sentinel-1 time series data for monitoring the phenology of winter wheat," *Remote Sens. Environ.*, vol. 246, Sep. 2020, Art. no. 111814, doi: 10.1016/j.rse.2020.111814.

[33] Z. Du et al., "Analysis of Landsat-8 OLI imagery for land surface water mapping," *Remote Sens. Lett.*, vol. 5, no. 7, pp. 672–681, Jul. 2014, doi: 10.1080/2150704X.2014.960606.

[34] W. Huang et al., "Automated extraction of surface water extent from Sentinel-1 data," *Remote Sens.*, vol. 10, no. 5, May 2018, Art. no. 797, doi: 10.3390/rs10050797.

[35] X. Yang, S. Zhao, X. Qin, N. Zhao, and L. Liang, "Mapping of urban surface water bodies from Sentinel-2 MSI imagery at 10 m resolution via NDWI-based image sharpening," *Remote Sens.*, vol. 9, no. 6, Jun. 2017, Art. no. 596, doi: 10.3390/rs9060596.

[36] F. Yao, J. Wang, C. Wang, and J.-F. Crétaux, "Constructing long-term high-frequency time series of global lake and reservoir areas using Landsat imagery," *Remote Sens. Environ.*, vol. 232, Oct. 2019, Art. no. 111210, doi: 10.1016/j.rse.2019.111210.

[37] N. Gorelick, M. Hancher, M. Dixon, S. Ilyushchenko, D. Thau, and R. Moore, "Google Earth Engine: Planetary-scale geospatial analysis for everyone," *Remote Sens. Environ.*, vol. 202, pp. 18–27, Dec. 2017, doi: 10.1016/j.rse.2017.06.031.

[38] E. Vermote, J. C. Roger, B. Franch, and S. Skakun, "LaSRC (Land Surface Reflectance Code): Overview, application and validation using MODIS, VIIRS, LANDSAT and Sentinel 2 data's," in *Proc. IEEE Int. Geosci. Remote Sens. Symp.*, 2018, pp. 8173–8176, doi: 10.1109/IGARSS.2018.8517622.

[39] Z. Zhu and C. Woodcock, "Object-based cloud and cloud shadow detection in landsat imagery," *Remote Sens. Environ.*, vol. 118, pp. 83–94, Mar. 2012, doi: 10.1016/j.rse.2011.10.028.

[40] T. D. Acharya, A. Subedi, and D. H. Lee, "Evaluation of water indices for surface water extraction in a Landsat 8 scene of Nepal," *Sensors*, vol. 18, no. 8, Aug. 2018, Art. no. 2580, doi: 10.3390/s18082580.

[41] H. K. Zhang et al., "Characterization of Sentinel-2A and Landsat-8 top of atmosphere, surface, and nadir BRDF adjusted reflectance and NDVI differences," *Remote Sens. Environ.*, vol. 215, pp. 482–494, Sep. 2018, doi: 10.1016/j.rse.2018.04.031.

[42] Y. Du, Y. Zhang, F. Ling, Q. Wang, W. Li, and X. Li, "Water bodies' mapping from Sentinel-2 imagery with modified normalized difference water index at 10-m spatial resolution produced by sharpening the SWIR band," *Remote Sens.*, vol. 8, no. 4, Apr. 2016, Art. no. 354, doi: 10.3390/rs8040354.
[43] H. Choi and J. Jeong, "Speckle noise reduction technique for SAR images using statistical characteristics of speckle noise and discrete wavelet transform," *Remote Sens.*, vol. 11, no. 10, Jan. 2019, Art. no. 1184, doi: 10.3390/rs11101184.
[44] G. Klogo, A. Gasonoo, and I. Ampomah, "On the performance of filters for reduction of speckle noise in SAR images off the coast of the gulf of Guinea," *Int. J. Inf. Technol. Model. Comput.*, vol. 1, pp. 43–52, Dec. 2013, doi: 10.5121/ijitmc.2013.1405.
[45] C. Liu, "Analysis of Sentinel-1 SAR data for mapping standing water in the Twente region," Masters thesis, Univ. Twente, Feb. 2016. Accessed: Mar. 3, 2023. [Online]. Available: https://webapps.itc.utwente.nl/librarywww/papers_2016/msc/wrem/cliu.pdf
[46] L. Ji, P. Gong, X. Geng, and Y. Zhao, "Improving the accuracy of the water surface cover type in the 30 m FROM-GLC product," *Remote Sens.*, vol. 7, no. 10, pp. 13507–13527, Oct. 2015, doi: 10.3390/rs71013507.
[47] S. Biancamaria, D. P. Lettenmaier, and T. M. Pavelsky, "The SWOT mission and its capabilities for land hydrology," *Surv. Geophys.*, vol. 37, no. 2, pp. 307–337, Mar. 2016, doi: 10.1007/s10712-015-9346-y.
[48] N. Qayyum, S. Ghuffar, H. M. Ahmad, A. Yousaf, and I. Shahid, "Glacial lakes mapping using multi satellite planetscope imagery and deep learning," *ISPRS Int. J. Geo-Inf.*, vol. 9, no. 10, Oct. 2020, Art. no. 560, doi: 10.3390/ijgi9100560.

Shahzaib Khan received the B.Tech. degree in civil engineering from the IIT Gandhinagar, Gujarat, India, in 2021. He is currently working toward the M.S. degree in civil and environmental engineering with the University of Washington, Seattle, WA, USA.

His research interests include remote sensing in the field of hydrology and citizen science.

Faisal Hossain received the B.S. degree in civil engineering from the National University of Singapore, Singapore, in 1996, the M.S. degree in environmental engineering from the IIT Varanasi, Varanasi, India, in 1999, and the Ph.D. degree in environmental engineering from the University of Connecticut, Storrs, CT, USA, in 2004.

He is currently a Professor with the Department of Civil and Environmental Engineering, University of Washington, Seattle, WA, USA. His research interests include hydrologic remote sensing, sustainable water resources engineering, transboundary water resources management, and engineering education.

Tamlin Pavelsky received the B.A. degree in geography from the Department of Geography, Middlebury College, Middlebury, VT, USA, in 2001, and the Ph.D. degree in geography from the University of California, Los Angeles, CA, USA, in 2008.

He is currently a Professor with the University of North Carolina, Chapel Hill, NC, USA, and the hydrology science lead for the Surface Water and Ocean Topography Mission.

Grant M. Parkins is currently a Watershed Education Coordinator with the Institute of the Environment, University of North Carolina, Chapel Hill, NC, USA.

Megan Rodgers Lane is the Public Science and Internship Coordinator with the Institute of Environment, University of North Carolina, Chapel Hill, NC, USA.

Angélica M. Gómez is currently a Research Scientist with the University of North Carolina, Chapel Hill, NC, USA.

Sanchit Minocha is currently working toward the Ph.D. degree in civil engineering with the Department of Civil and Environmental Engineering, University of Washington, Seattle, WA, USA.

Pritam Das is currently working toward the Ph.D. degree in civil engineering with the Department of Civil and Environmental Engineering, University of Washington, Seattle, WA, USA.

Sheikh Ghafoor is currently a Professor with the Tennessee Technological University, Cookeville, TN, USA.

Md. Arifuzzaman Bhuyan received the B.S. degree in civil engineering from the Bangladesh University of Engineering and Technology, Dhaka, Bangladesh, in 2004.

He is currently an Engineer with the Bangladesh Water Development Board, Dhaka, Bangladesh.

Md. Nazmul Haque is currently an Engineer with the Bangladesh Water Development Board, Dhaka, Bangladesh.

Preetom Kumar Sarker is currently an Engineer with the Bangladesh Water Development Board, Dhaka, Bangladesh.

Partho Protim Borua is currently an Engineer with the Bangladesh Water Development Board, Dhaka, Bangladesh.

Jean-Francois Cretaux is currently a Scientist with the Laboratoire d'Études en Géophysique et Océanographie Spatiales, Toulouse, France. He is also the hydrology science lead for the Surface Water and Ocean Topography (SWOT) Mission.

Nicolas Picot is currently a Scientist with the Centre National d'Etudes Spatiales, Paris, France.

Vivek Balakrishnan is currently a Scientist with the Centre for Water Resources Development and Management, Kerala, India.

Shakeel Ahmad is currently a Scientist with the Aligarh Muslim University, Aligarh, India.

Nirakar Thapa is currently a Scientist with the Department of Hydrology and Meteorology, Kathmandu, Nepal.

Rajan Bhattarai is currently a Deputy Director with the Department of Hydrology and Meteorology, Kathmandu, Nepal.

Faizan-ul Hasan is currently a Scientist with the Pakistan Council of Research in Water Resources, Islamabad, Pakistan.

Bareerah Fatima is currently a Scientist with the Pakistan Council of Research in Water Resources, Islamabad, Pakistan.

Muhammad Ashraf is currently the Chairman of the Pakistan Council of Research in Water Resources, Islamabad, Pakistan.

Shahryar Khalique Ahmad is currently a Research Scientist with the Goddard Space Flight Center Hydrological Sciences Branch, Greenbelt, MD, USA.

Arthur Compin is currently a Scientist with the University of Toulouse, Toulouse, France.